

Convergence of redundancy-free spiking neural networks to rate networks

Valentin Schmutz, Johanni Brea, Wulfram Gerstner

Laboratory of Computational Neuroscience, École Polytechnique Fédérale de Lausanne, 1015 Lausanne, Switzerland

Can the dynamics of large Spiking Neural Networks (SNNs) converge to the smooth dynamics of equally large Recurrent Neural Networks (RNNs)? Classical mean-field theory provides a positive answer when the networks are redundant, that is, when each neuron has many “twins” receiving nearly identical inputs. Using a disordered network model which guarantees the absence of redundancy in large networks, we show that redundancy-free, densely connected spiking neural networks converge to RNNs when the ℓ^2 norms of the rows of the connectivity matrix tend to zero.

Neurons in the brain interact via spikes – short and stereotyped membrane potential deflections – commonly modeled as Dirac pulses [1]. SNNs with recurrent connectivity offer simplified models of real networks retaining the essential biological feature of spike-based neuronal communication. On the other hand, traditional RNNs are continuous dynamical systems where abstract rate neurons directly transmit their firing rate to other neurons, a type of communication which is not biological. Despite their inferior realism, RNNs continue to play a central role in theoretical neuroscience because they can be trained by modern machine learning methods [2–4], they can be analysed using tools from statistical physics [5–8], and because biological networks are believed to perform computation by implementing continuous dynamical systems [9, 10]. Closing the gap between the more biological SNNs and the more tractable RNNs requires identifying the conditions under which the continuous dynamics of RNNs can be approximated by SNNs [11].

To clearly state the problem, let us consider an SNN composed of N Poisson neurons (linear-nonlinear-Poisson neurons [12] or nonlinear Hawkes processes [13]). For each neuron index i , the spike times $\{t_i^k\}_k$ of neuron i , which define the neuron’s spike train $S_i(t) = \sum_k \delta(t - t_i^k)$, are generated by an inhomogeneous Poisson process with instantaneous firing rate $\phi(h_i(t))$, where $h_i(t)$ represents the neuron’s potential and ϕ is a positive-valued nonlinear transfer function. The potential $h_i(t)$ is a leaky integrator of the recurrent inputs coming from neurons $j \neq i$ and the external input $I_i^{\text{ext}}(t)$:

$$\tau \frac{d}{dt} h_i(t) = -h_i(t) + \sum_{j=1}^N J_{ij} S_j(t) + I_i^{\text{ext}}(t), \quad (1)$$

where τ is the integration (or membrane) time constant and J_{ij} is the synaptic weight from neuron j to neuron i (by convention, $J_{ii} = 0$). While the spike-based model described here is biologically simplistic, it is mathematically convenient as it has a straightforward rate-based counterpart. If we replace the spike trains $\{S_j(t)\}_j$ in Eq. (1) by the corresponding instantaneous firing rates $\{\phi(h_j(t))\}_j$ (i.e. neurons communicate their firing rate

directly), we get the rate-based dynamics

$$\tau \frac{d}{dt} x_i(t) = -x_i(t) + \sum_{j=1}^N J_{ij} \phi(x_j(t)) + I_i^{\text{ext}}(t), \quad (2)$$

which defines a RNN with N rate units. To avoid confusion, we write $h_i(t)$ for the potentials of the SNN (1) and $x_i(t)$ for the potentials of the RNN (2). While the mapping from the SNN to the RNN looks simple at first glance, the spike-based stochastic process Eq. (1) and the rate-based dynamical system Eq. (2) describe very different kinds of systems and the SNN potentials $h_i(t)$ are not guaranteed, in general, to be equal or even close to the RNN potentials $x_i(t)$ even if both networks receive the same external input. Note that if the neurons are uncoupled (i.e. $J_{ij} = 0$ for all i, j), the SNN potentials $h_i(t)$ are trivially equal to the RNN potentials $x_i(t)$. Therefore, comparing the SNN and the RNN is meaningful only if the coupling does not vanish. For nontrivial coupling, there are two known types of scaling limits where the SNN potentials $h_i(t)$ converge to the RNN potentials $x_i(t)$:

- (i) *Spatial averaging over many redundant neurons:* Consider networks of increasing size N . If each neuron can be assigned to a point in some fixed space such that two neurons assigned to the same point always share the same recurrent and external input, and if the synaptic weights are scaled by $1/N$, we can take the mean-field limit $N \rightarrow \infty$ [14, 15]. The fixed space can be either discrete and finite [16, 17] or continuous and finite-dimensional [18], e.g. a ring. These classical mean-field limits entail redundancy, i.e. the existence of large groups of identical neurons receiving the same recurrent and external input when $N \rightarrow \infty$. To our knowledge, this form of redundancy has not been found in the cortex.
- (ii) *Temporal averaging over many spikes:* In Eq. (1), we can replace the transfer function ϕ and the synaptic weights $\{J_{ij}\}_{i \neq j}$ by $b \phi$ and $\{J_{ij}/b\}_{i \neq j}$, respectively (for $b > 0$), and take the limit $b \rightarrow \infty$ [19]. This limit entails arbitrarily high firing rates in the SNN, which is biologically unrealistic since two spikes have to be separated by at least 1 to 2 milliseconds

(the absolute refractory period) [20]. Similarly, we can take the limit $\tau \rightarrow \infty$ in both Eq. (1) and (2) while re-scaling the synaptic weights $\{J_{ij}\}_{i \neq j}$ and the external inputs $I_i^{\text{ext}}(t)$ by $1/\tau$. This last limit entails arbitrarily slow network dynamics, which is incompatible with human visual processing speed (less than 150 milliseconds) [21].

In this letter, we address the following question: can large SNNs, as defined in Eq. (1), converge to equally large RNNs without involving redundancy or temporal averaging.

Avoiding temporal averaging (ii) will be guaranteed by assuming that $\max \phi \leq 1/\tau$. Under this condition, leaky integration by the potential, Eq. (1), is too fast to average out the Poisson noise of individual input spike trains and neither of the two scalings mentioned under (ii) can be applied.

To assess the redundancy of an RNN, we look at the distribution of correlations between pairs of distinct neurons $i \neq j$

$$\rho(x_i, x_j) := \lim_{T \rightarrow \infty} \frac{1}{T} \int_0^T \frac{(x_i(t) - \bar{x}_i)(x_j(t) - \bar{x}_j)}{\sigma_{x_i} \sigma_{x_j}} dt,$$

where \bar{x}_i and $\sigma_{x_i}^2$ are, respectively, the time average and fluctuation of $x_i(t)$:

$$\begin{aligned} \bar{x}_i &:= \lim_{T \rightarrow \infty} \frac{1}{T} \int_0^T x_i(t) dt, \\ \sigma_{x_i}^2 &:= \lim_{T \rightarrow \infty} \frac{1}{T} \int_0^T (x_i(t) - \bar{x}_i)^2 dt. \end{aligned} \quad (3)$$

Based on the correlation distribution (which has total mass 1), we say that a network is redundant if the mass of the correlation distribution around 1 (e.g. on some small interval $[\theta, 1]$ with $0 < \theta < 1$) is non-negligible. For example, if the N units of a RNN are uniformly assigned to points on a ring where nearby neurons receive similar recurrent and external (stochastic) inputs, in the mean-field limit $N \rightarrow \infty$, the distribution of the correlations $\{\rho(x_i, x_j)\}_{i \neq j}$ converge to a correlation distribution with strictly positive mass around at 1, reflecting the fact that the number of redundant “twins” per unit grows linearly with N (Fig 1A, see the Appendix for the details on the simulated model). This simple ring model illustrates how redundancy builds up in classical mean-field models as $N \rightarrow \infty$ (i).

Conversely, we say that large networks of a given model are *redundancy-free* if, for any $0 < \theta < 1$, the mass of the correlation distribution on the interval $[\theta, 1]$ vanishes as $N \rightarrow \infty$. In the following, we propose a disordered network model where large networks are redundancy-free.

Input-driven disordered network model.— We construct the connectivity matrix $\mathbf{J} = \{J_{ij}\}_{i,j}$ as a sum of random rank-one matrices (minus self-interaction terms), a construction similar to that of Hopfield networks [7, 22, 23].

For any number of units N and any number of patterns p , let ξ be a random $N \times p$ -matrix with *i.i.d.*, zero-mean, unit-variance, normally distributed entries $\{\xi_{i\mu}\}_{i,\mu}$. We choose a connectivity matrix given by

$$J_{ij} := \frac{1}{cN} \sum_{\mu=1}^p \xi_{i\mu} (\phi(\xi_{j\mu}) - a) \quad \text{for all } i \neq j, \quad (4)$$

and $J_{ii} := 0$ for all i , where the constants $a := \int_{-\infty}^{\infty} \mathcal{D}z \phi(z)$ and $c := \int_{-\infty}^{\infty} \mathcal{D}z (\phi(z) - a)^2$, $\mathcal{D}z$ denoting the standard Gaussian measure, guarantee the normalization

$$\frac{1}{cN} \sum_{i=1}^N (\phi(\xi_{i1}) - a) \phi(\xi_{i1}) \rightarrow 1, \quad \text{as } N \rightarrow \infty.$$

A well-known feature of this type of connectivity is that, exchanging the order of summation, the dynamics of the RNN (2) can be re-written in terms of p overlap variables $\{m_\mu(t)\}_\mu$ [24–26]: for all $i = 1, \dots, N$ and for all $\mu = 1, \dots, p$,

$$\begin{aligned} \tau \frac{d}{dt} x_i(t) &= -x_i(t) + \sum_{\nu=1}^p \xi_{i\nu} m_\nu(t) - \gamma_i \phi(x_i(t)) + I_i^{\text{ext}}(t), \\ m_\mu(t) &= \frac{1}{cN} \sum_{j=1}^N (\phi(\xi_{j\mu}) - a) \phi(x_j(t)), \end{aligned}$$

where the $\gamma_i := \frac{1}{cN} \sum_{\nu=1}^p \xi_{i\nu} (\phi(\xi_{i\nu}) - a)$ are virtual self-interaction weights. Analogously, for the SNN, we have

$$\begin{aligned} \tau \frac{d}{dt} h_i(t) &= -h_i(t) + \sum_{\nu=1}^p \xi_{i\nu} m_\nu(t) - \gamma_i S_i(t) + I_i^{\text{ext}}(t), \\ m_\mu(t) &= \frac{1}{cN} \sum_{j=1}^N (\phi(\xi_{j\mu}) - a) S_j(t). \end{aligned} \quad (5)$$

This reformulation clearly shows that if $p \ll N$, the γ_i are small and therefore the recurrent drive $\{\sum_{j=1}^N J_{ij} \phi(x_j(t))\}_i$ is approximately restricted to the p -dimensional subspace spanned by the p columns of the random matrix ξ . To force the recurrent drive to visit all p dimensions homogeneously over time in a single stationary process, we inject the following p -dimensional external input to half of the neurons:

$$\begin{aligned} I_i^{\text{ext}}(t) &= \frac{\sigma}{\sqrt{p}} \sum_{\mu=1}^p \xi_{i\mu} \eta_\mu(t) & \text{if } i \leq N/2, \\ I_i^{\text{ext}}(t) &= 0 & \text{if } i > N/2, \end{aligned} \quad (6)$$

where the $\eta_1(t), \dots, \eta_p(t)$ are independent Gaussian white noises and $\sigma > 0$ is the input noise parameter. For indexing convenience, the potentials of the $N/2$ neurons receiving no external input but only recurrent input will

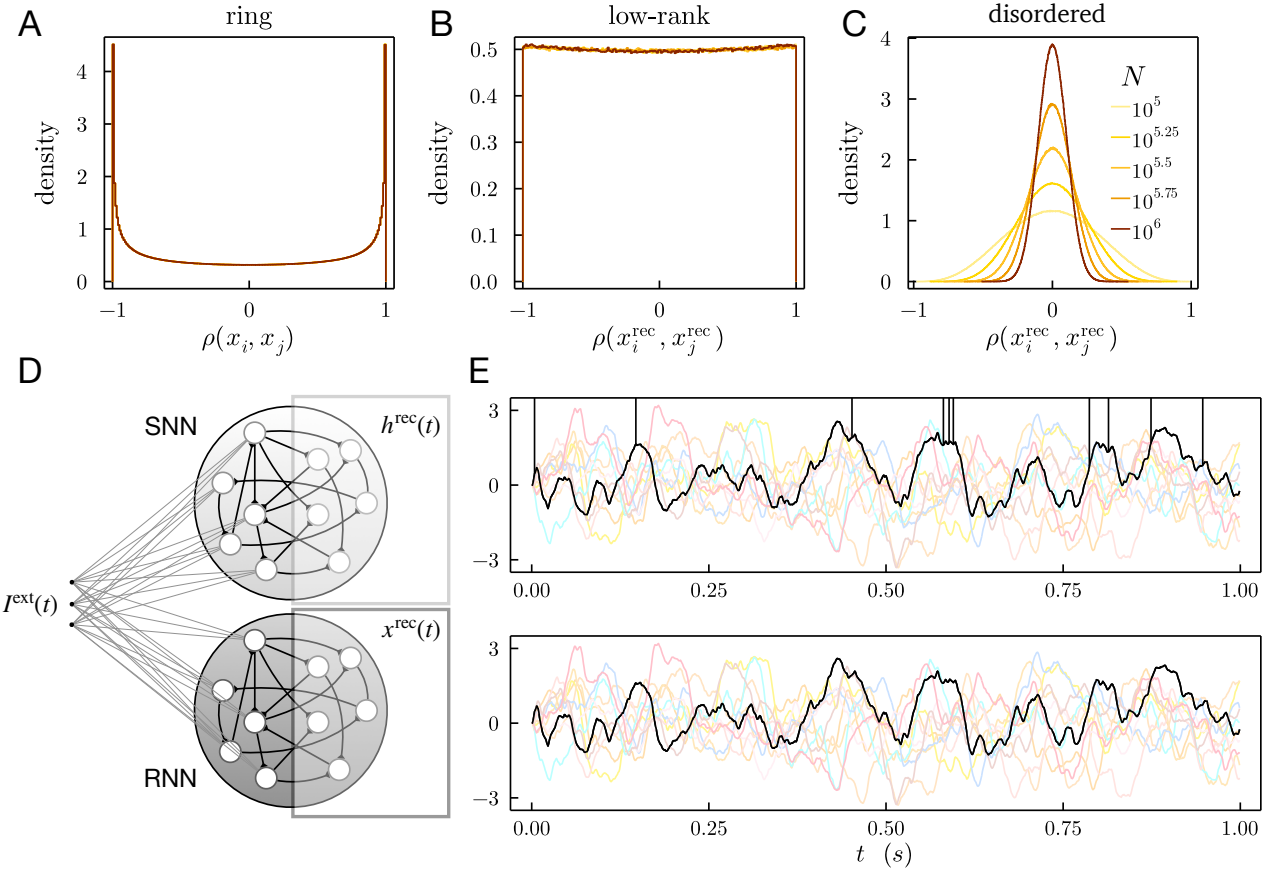


FIG. 1. Networks with (A,B) and without (C) redundant neurons. Distributions of correlations $\rho(x_i, x_j)$ in RNNs of increasing size N , for (A) a ring model, (B) a low-rank model with rank $p = 3$, and (C) a disordered network model with load $\alpha = 10^{-4}$. In (B,C), the correlations $\rho(x_i^{\text{rec}}, x_j^{\text{rec}})$ are for pairs of neurons receiving no external input but only recurrent input. In the disordered network model (C), correlations concentrate around 0 as $N \rightarrow \infty$. (D) SNN and RNN comparison. The potentials of the neurons receiving no external input but only recurrent input, $h^{\text{rec}}(t)$ and $x^{\text{rec}}(t)$, are linear readouts of the recurrent drive. (E) Trajectories of single-neuron potentials in the SNN ($h_i^{\text{rec}}(t)$, upper panel) and in the RNN ($x_i^{\text{rec}}(t)$, lower panel) during a one-second simulation of the setup shown in (D). The networks have $N = 10^6$ neurons and load $\alpha = 10^{-4}$, as in (C). The same randomly chosen 11 neurons are recorded in the SNN and in the RNN and each color corresponds to a different neuron index i (the colors in the upper and lower panels correspond). For one neuron index i (the black trace), the spike times of the neuron in the SNN are indicated by vertical bars. The differences between the potentials of the SNN and the RNN are almost imperceptible. (A-E) Neuronal parameters: $\tau = 10$ ms and $\phi(x) = \frac{1}{2\tau}(\tanh(x - \theta) + 1)$ with $\theta = 2$. Input noise is $\sigma = 0.5$ in (B-E).

be denoted $x_i^{\text{rec}}(t)$; the $x_i^{\text{rec}}(t)$ can therefore be seen as linear readouts of the recurrent drive; cf. Eq. (2).

If the number of patterns p is kept constant as $N \rightarrow \infty$, the limit RNN is a low-rank mean-field model [8]. In such a low-rank model, redundancy also builds up as $N \rightarrow \infty$, namely, the distribution of correlations converges to a limit distribution where the density at 1 is strictly positive (Fig. 1B), indicating again that the number of redundant “twins” per unit grows linearly with N . The reason for the accumulation of redundancy is the same as in the ring model except that, here, the fixed space is not a ring but \mathbb{R}^p : unit i has coordinate $\xi_i = (\xi_{i1}, \dots, \xi_{ip})$ and units with similar coordinates receive similar recurrent and external inputs. Therefore, if p is kept constant as

$N \rightarrow \infty$, we fall again in the case of spatial averaging over redundant neurons (i). Actually, the population dynamics can be exactly described by a neural field equation [27].

To prevent redundancy from accumulating as $N \rightarrow \infty$, we make the number of patterns p grow linearly with N , taking $p = \alpha N$ for some fixed load $\alpha > 0$, as in the Hopfield model [23]. With this choice of scaling, synaptic weights $\{J_{ij}\}_{i,j}$ scale as $\mathcal{O}(1/\sqrt{N})$ (as in random RNNs [6, 28]), whence the name “disordered network” for this model. We will show that for any fixed $\alpha > 0$, large networks are redundancy-free (as defined above). Then, we will show that large SNNs converge to large RNNs, as $\alpha \rightarrow 0$, achieving the numerical demonstration that large, redundancy-free SNNs can converge to equally large

RNNs. To show the convergence of the SNN (1) to the RNN (2), we will inject the same time-dependent external input (6) in both networks (Fig 1D) and compare the trajectories $h_i^{\text{rec}}(t)$ of the SNN with the trajectories $x_i^{\text{rec}}(t)$ of the RNN (Fig 1E).

We first verify numerically that the SNNs (and the RNNs) converge to the dynamic mean-field limit of a disordered system [6] (not to be confused with classical mean-field limits where there is no disorder [15, 29]). Since the trajectories $h_i^{\text{rec}}(t)$ of the SNN are almost identical to the trajectories $x_i^{\text{rec}}(t)$ of the RNN when α is small ($\alpha = 10^{-4}$ in Fig. 1C,E and Fig 2A-E), we only show numerical results for the SNN; those for the RNN are almost identical. Defining the time average \bar{h}_i^{rec} and the fluctuation $\sigma_{h_i^{\text{rec}}}$ as in Eq. (3), we see that the distributions of \bar{h}_i^{rec} concentrate around 0 (Fig 2A) and the distributions of $\sigma_{h_i^{\text{rec}}}$ concentrate around a value slightly larger than 1 (Fig 2B) as $N \rightarrow \infty$. Moreover, when N is large, the trajectories $h_i^{\text{rec}}(t)$ (and $x_i^{\text{rec}}(t)$) look like independent realizations of the same stochastic process (Fig. 1E), which is reminiscent of the dynamic mean-field theory of random chaotic RNNs [6, 28]. The comprehensive study of this putative dynamic mean-field theory is beyond the scope of this letter.

Large networks are redundancy-free.— To explain why, in the disordered network model described above, correlations concentrate around 0 as $N \rightarrow \infty$ (Fig. 1C), we first verify numerically that the recurrent drive of the SNN is of dimension $p = \alpha N$ by performing a principal component analysis (PCA) of the trajectories $h_i^{\text{rec}}(t)$ over a single trial of 100 s. The result shows that the cumulative explained variance grows approximately linearly with the PC dimension and saturates at p (Fig. 2C), confirming that the recurrent drive homogeneously visits all p dimensions spanned by the columns of ξ . This implies that the overlaps, Eq. (5), also homogeneously visit their p dimensions. In the overlap formulation of the dynamics of the SNN, Eq. (5), we see that, when α is small, the recurrent inputs of two distinct neurons i and j are approximately $\sum_{\mu=1}^p \xi_{i\mu} m_{\mu}(t)$ and $\sum_{\mu=1}^p \xi_{j\mu} m_{\mu}(t)$ respectively. Therefore, for large N , we expect the correlations between distinct neurons to approximate the correlations between the corresponding rows of ξ [30]:

$$\rho(h_i^{\text{rec}}, h_j^{\text{rec}}) \approx \frac{1}{p} \sum_{\mu=1}^p \xi_{i\mu} \xi_{j\mu}. \quad (7)$$

The approximation Eq. (7) implies that the distribution of correlations converges to a zero-mean normal distribution with variance $1/p$, which we confirm numerically (Fig. 2D). Since $p = \alpha N$, the fact that the normal distribution has variance $1/p$ is sufficient to guarantee the absence of redundancy as $N \rightarrow \infty$ (i). Indeed, for any $0 < \theta < 1$, the expected number of pairs of distinct neurons having a correlation greater or equal to θ is the product of the proportion of such pairs and the total number of pairs

in the network. This product can be upper-bounded by $e^{-\theta^2 p/2} \cdot N(N-1)/2$ (using a standard Gaussian tail bound) and therefore converges to 0 as $N \rightarrow \infty$ (since $p = \alpha N$).

Large SNNs converge to large RNNs as $\alpha \rightarrow 0$.— Finally, we study the convergence of the SNN to the RNN as $\alpha \rightarrow 0$. Let us first observe that, for a fixed $\alpha > 0$ and as $N \rightarrow \infty$, the distributions of the single-neuron distances

$$\Delta_i^{\text{rec}} := \lim_{T \rightarrow \infty} \int_0^T |h_i^{\text{rec}}(t) - x_i^{\text{rec}}(t)| dt.$$

concentrate around a finite value (around 0.03 for $\alpha = 10^{-4}$, Fig. 2E). Thereby, for any $\alpha > 0$, we can define the $N \rightarrow \infty$ limit distance between the SNN and the RNN as the time average of the distance between the potential of a *typical* neuron i^* (receiving recurrent input only) in the limit SNN, $\hat{h}_{i^*}^{\text{rec}}(t)$, and the potential of the corresponding rate unit in the limit RNN, $\hat{x}_{i^*}^{\text{rec}}(t)$:

$$\Delta^{\text{rec}}(\alpha) := \lim_{T \rightarrow \infty} \frac{1}{T} \int_0^T |\hat{h}_{i^*}^{\text{rec}}(t) - \hat{x}_{i^*}^{\text{rec}}(t)| dt.$$

Numerical estimates of the limit distance $\Delta^{\text{rec}}(\alpha)$ indeed show that the limit SNN converges to the limit RNN as $\alpha \rightarrow 0$ and the power law fit of the estimated $\Delta^{\text{rec}}(\alpha)$ (Fig. 2F) indicates that

$$\Delta^{\text{rec}}(\alpha) = \mathcal{O}(\sqrt{\alpha}), \quad \text{as } \alpha \rightarrow 0. \quad (8)$$

We have therefore shown, using the input-driven disordered network model, that large SNNs can converge to equally large RNNs (i) without redundancy and (ii) temporal averaging. In the absence of redundancy, what mechanism allows an SNN to approximate an RNN? Borrowing ideas from an established mean-field convergence proof technique [16, 31] (see also [32]), we present a heuristic argument suggesting that the convergence of the SNNs to the RNNs is related to the ℓ^2 norms (Euclidean norms) of the incoming synaptic weights to each neuron (the rows of the connectivity matrix) $\|\mathbf{J}_i\|_2 = \sqrt{\sum_{j=1}^N J_{ij}^2}$.

For simplicity, let us assume that at some initial time t , $h_i(t) = x_i(t)$, for all $i = 1, \dots, N$. Since the SNN (1) and the RNN (2) receive the same external input $I_i^{\text{ext}}(t)$, for a small time step dt , we have, for the expected difference between Eqs. (1) and (2),

$$\begin{aligned} & \mathbb{E} [|h_i(t+dt) - x_i(t+dt)|] \\ &= \frac{1}{\tau} \mathbb{E} \left[\left| \sum_{j=1}^N J_{ij} n_j - \sum_{j=1}^N J_{ij} \phi(x_j(t)) dt \right| \right] + o(dt), \end{aligned}$$

where the $\{n_j\}_j$ are independent Poisson-distributed random variables with means $\{\phi(h_j(t))dt\}_j \equiv \{\phi(x_j(t))dt\}_j$.

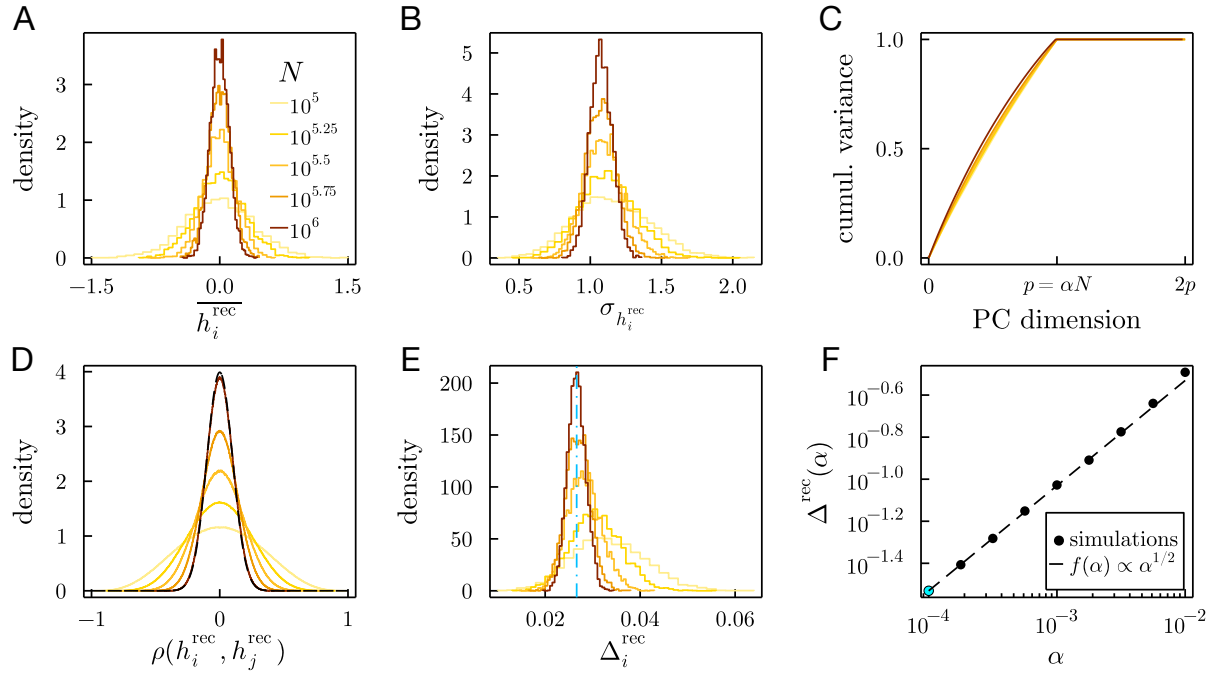


FIG. 2. (A-E) Scaling behavior of the disordered SNN as N increases for load $\alpha = 10^{-4}$. (A) Distributions of single-neuron average potentials \bar{h}_i^{rec} in the SNNs concentrate around 0. (B) Distributions of single-neuron potential fluctuations $\sigma_{h_i^{\text{rec}}}$ concentrate around a value slightly larger than 1. (C) Principal component analysis of $h_i^{\text{rec}}(t)$. The recurrent drive spans the whole $p = \alpha N$ -dimensional subspace. (D) Distributions of correlations $\rho(h_i^{\text{rec}}, h_j^{\text{rec}})$. The dashed black line represents a centered normal distribution with variance $1/p$, for $N = 10^6$. As in Fig. 1C, correlations concentrate around 0. (E) Distributions of single-neuron distances Δ_i^{rec} . Distances concentrate around a limit distance $\Delta(\alpha) \approx 0.03$ (dashed blue line). (F) Numerical estimate of the limit distance $\Delta(\alpha)$ (circles) and fitted power law with exponent $1/2$ (dashed line). The value $\Delta^{\text{rec}}(\alpha)$ for $\alpha = 10^{-4}$ is indicated by a blue circle and corresponds to the dashed blue line in (E). (A-F) All the quantities are estimated using samples of 5000 neurons. Same neuronal and noise parameters as in Fig. 1B-E.

By Jensen's inequality and the independence of the random variables $\{n_j\}_j$, we get the bound

$$\mathbb{E} \left[\left| \sum_{j=1}^N J_{ij} n_j - \sum_{j=1}^N J_{ij} \phi(x_j(t)) dt \right|^2 \right] \leq \sum_{j=1}^N J_{ij}^2 \phi(x_j(t)) dt.$$

Since the transfer function ϕ is upper-bounded by $1/\tau$, we get

$$\mathbb{E} [|h_i(t+dt) - x_i(t+dt)|] \leq \frac{1}{\tau} \|\mathbf{J}_i\|_2 \sqrt{\frac{dt}{\tau}} + o(dt). \quad (9)$$

The bound (9) implies that if for all i the ℓ^2 norm of the incoming synaptic weights, $\|\mathbf{J}_i\|_2$, is small, then the distance between the SNN (1) and the RNN (2) remains small, at least over a short time [33]. In our disorder network model, the reason why the distance between the SNN and the RNN does not diverge over time is likely due to the fact that we are in an input-driven regime.

Importantly, the bound (9), which holds for any arbitrary connectivity matrix \mathbf{J} , is consistent with the idea that spike noise absorption in large networks – enabling a stochastic SNN to behave like a deterministic RNN – does

not require redundancy (as we have numerically shown with our the disordered network example).

Classical mean-field limit results where synaptic weights are scaled by $1/N$ (i), e.g. for interacting homogeneous populations [14, 15] or spatially structured networks [15], can be rigorously proven using bounds similar to Eq. (9) [16–18, 34, 35]. Indeed, if weights are scaled by $1/N$, then $\|\mathbf{J}_i\|_2^2 = \mathcal{O}(1/N)$ and the bound (9) tends to 0 as $N \rightarrow \infty$ (see [16–18] for full mean-field limit convergence proofs).

By contrast, in the case of our disordered network model, the synaptic weights $\{J_{ij}\}_{i \neq j}$ defined in Eq. (4) scale as $\mathcal{O}(1/\sqrt{N})$ and the distribution of the ℓ^2 norms $\|\mathbf{J}_i\|_2$ concentrate around $\sqrt{\alpha/c}$ [36], meaning that for a typical neuron i^* in a large network, $\|\mathbf{J}_{i^*}\|_2 = \sqrt{\alpha/c}$. Hence, as $\alpha \rightarrow 0$, the limit distance between a large SNN and a large RNN $\Delta^{\text{rec}}(\alpha)$, Eq. (8), tends to zero at the same speed as the ℓ^2 norm $\|\mathbf{J}_{i^*}\|_2$, which supports the claim that the bound (9) explains (at least heuristically) spike noise absorption in redundancy-free networks. Whereas classical mean-field models rely on redundancy and the law of large numbers to absorb spike noise, the bound (9) suggests that the “independence” of neurons and the concentration of measure phenomenon (which

only require variables to be independent [37]) are sufficient for redundancy-free networks to absorb spike noise; this heuristic observation should be confirmed by future mathematical proofs (see [32] for a first step).

More generally, absorbing spike noise by imposing small ℓ^2 norms $\|\mathbf{J}_i\|_2$ (see Eq. (9)) while keeping a nontrivial recurrent drive requires networks to be densely connected (fixed *fraction* of nonzero incoming synaptic weights as $N \rightarrow \infty$), as opposed to sparsely connected (fixed *number* of nonzero incoming synaptic weights as $N \rightarrow \infty$) [38, 39]. Note however that not all densely connected networks absorb spike noise. For example, in random chaotic networks [6], the ℓ^2 norms $\|\mathbf{J}_i\|_2$ are not small and spike noise is not absorbed [40]. This shows how the ℓ^2 norms of the incoming synaptic weights can help distinguish spike noise-absorbing dense networks, which approximate rate-based dynamics, from dense networks where spike noise plays a significant role in network dynamics.

While the disordered network models considered here are redundancy-free, it can be argued that they are redundant in a weaker sense: the dimensionality $p = \alpha N$ of the recurrent drive has to be small in proportion to the number of neurons N for the SNN to approximate the RNN. Our disordered network model therefore shows a trade-off between spike noise absorption and the dimensionality of noise-robust recurrent dynamics. Whether this trade-off is a general feature of spiking neural networks is an open theoretical question we leave for future work. Such a tradeoff could shed light on how the noisy wetware of the brain [41] constrains the implementation of “computation through neural population dynamics” [10].

This Research is supported by the Swiss National Science Foundation (grant no 200020_207426).

-
- [1] W. Gerstner and W. M. Kistler, *Spiking neuron models: Single neurons, populations, plasticity* (Cambridge university press, 2002).
- [2] P. J. Werbos, Backpropagation through time: what it does and how to do it, *Proceedings of the IEEE* **78**, 1550 (1990).
- [3] D. Sussillo and O. Barak, Opening the black box: low-dimensional dynamics in high-dimensional recurrent neural networks, *Neural computation* **25**, 626 (2013).
- [4] O. Barak, Recurrent neural networks as versatile tools of neuroscience research, *Current opinion in neurobiology* **46**, 1 (2017).
- [5] D. J. Amit, H. Gutfreund, and H. Sompolinsky, Storing infinite numbers of patterns in a spin-glass model of neural networks, *Physical Review Letters* **55**, 1530 (1985).
- [6] H. Sompolinsky, A. Crisanti, and H.-J. Sommers, Chaos in random neural networks, *Physical review letters* **61**, 259 (1988).
- [7] U. Pereira and N. Brunel, Attractor dynamics in networks with learning rules inferred from in vivo data, *Neuron* (2018).
- [8] F. Mastrogiovanni and S. Ostoicic, Linking connectivity, dynamics, and computations in low-rank recurrent neural networks, *Neuron* **99**, 609 (2018).
- [9] K. V. Shenoy, M. Sahani, M. M. Churchland, *et al.*, Cortical control of arm movements: a dynamical systems perspective, *Annu Rev Neurosci* **36**, 337 (2013).
- [10] S. Vyas, M. D. Golub, D. Sussillo, and K. V. Shenoy, Computation through neural population dynamics, *Annual Review of Neuroscience* **43**, 249 (2020).
- [11] R. Brette, Philosophy of the spike: rate-based vs. spike-based theories of the brain, *Frontiers in systems neuroscience* **9**, 151 (2015).
- [12] E. Chichilnisky, A simple white noise analysis of neuronal light responses, *Network: computation in neural systems* **12**, 199 (2001).
- [13] P. Brémaud and L. Massoulié, Stability of nonlinear Hawkes processes, *Ann. Probab.* **24**, 1563 (1996).
- [14] W. Gerstner and J. L. van Hemmen, Associative memory in a network of ‘spiking’neurons, *Netw. Comput. Neural Syst.* **3**, 139 (1992).
- [15] W. Gerstner, Time structure of the activity in neural network models, *Phys. Rev. E* **51**, 738 (1995).
- [16] S. Delattre, N. Fournier, and M. Hoffmann, Hawkes processes on large networks, *Ann. Appl. Probab.* **26**, 216 (2016).
- [17] S. Ditlevsen and E. Löcherbach, Multi-class oscillating systems of interacting neurons, *Stochastic Process. Appl.* **127**, 1840 (2017).
- [18] J. Chevallier, A. Duarte, E. Löcherbach, and G. Ost, Mean field limits for nonlinear spatially extended hawkes processes with exponential memory kernels, *Stochastic Processes and their Applications* **129**, 1 (2019).
- [19] T. G. Kurtz, Limit theorems for sequences of jump markov processes approximating ordinary differential processes, *Journal of Applied Probability* **8**, 344 (1971).
- [20] E. R. Kandel, J. H. Schwartz, T. M. Jessell, S. Siegelbaum, A. J. Hudspeth, S. Mack, *et al.*, *Principles of neural science*, Vol. 4 (McGraw-hill New York, 2000).
- [21] S. Thorpe, D. Fize, and C. Marlot, Speed of processing in the human visual system, *nature* **381**, 520 (1996).
- [22] J. J. Hopfield, Neural networks and physical systems with emergent collective computational abilities, *Proceedings of the national academy of sciences* **79**, 2554 (1982).
- [23] D. J. Amit, H. Gutfreund, and H. Sompolinsky, Spin-glass models of neural networks, *Physical Review A* **32**, 1007 (1985).
- [24] D. J. Amit, *Modeling brain function: The world of attractor neural networks* (Cambridge university press, 1989).
- [25] J. Hertz, A. Krogh, and R. G. Palmer, *Introduction to the theory of neural computation* (1991).
- [26] W. Gerstner, W. M. Kistler, R. Naud, and L. Paninski, *Neuronal dynamics: From single neurons to networks and models of cognition* (Cambridge University Press, 2014).
- [27] See Supplementary Materials “From low-rank SNNs to neural field equations”.
- [28] M. Helias and D. Dahmen, *Statistical Field Theory for Neural Networks* (Springer, 2020).
- [29] W. Gerstner, Population dynamics of spiking neurons: fast transients, asynchronous states, and locking, *Neural Comput.* **12**, 43 (2000).
- [30] For additional explanations, see Supplementary Materials “Feedforward network approximation”.
- [31] A.-S. Sznitman, Topics in propagation of chaos, in *École d’Été de Probabilités de Saint-Flour XIX—1989*, Lecture

- Notes in Math., Vol. 1464 (Springer, Berlin, 1991) pp. 165–251.
- [32] P.-E. Jabin, D. Poyato, and J. Soler, Mean-field limit of non-exchangeable systems, arXiv preprint arXiv:2112.15406 (2021).
- [33] In the Supplementary Materials, using a feedforward network approximation of the input-driven SNNs and the RNNs, we show, heuristically, why the distance remains small over an arbitrarily long time and why the time average distance $\Delta^{\text{rec}}(\alpha)$ scales as $\mathcal{O}(\sqrt{\alpha})$ as $\alpha \rightarrow 0$.
- [34] N. Fournier and E. Löcherbach, On a toy model of interacting neurons, in *Annales de l'Institut Henri Poincaré, Probabilités et Statistiques*, Vol. 52 (Institut Henri Poincaré, 2016) pp. 1844–1876.
- [35] J. Chevallier, Mean-field limit of generalized Hawkes processes, *Stochastic Process. Appl.* **127**, 3870 (2017).
- [36] See Supplementary Materials “Concentration of the ℓ^2 norms of the incoming weights” for the detailed calculations.
- [37] M. Talagrand, A new look at independence, *The Annals of probability* , 1 (1996).
- [38] N. Brunel and V. Hakim, Fast global oscillations in networks of integrate-and-fire neurons with low firing rates, *Neural computation* **11**, 1621 (1999).
- [39] N. Brunel, Dynamics of sparsely connected networks of excitatory and inhibitory spiking neurons, *Journal of computational neuroscience* **8**, 183 (2000).
- [40] A. van Meegen and S. J. van Albada, Microscopic theory of intrinsic timescales in spiking neural networks, *Physical Review Research* **3**, 043077 (2021).
- [41] A. A. Faisal, L. P. Selen, and D. M. Wolpert, Noise in the nervous system, *Nature reviews neuroscience* **9**, 292 (2008)

Supplemental Materials: Convergence of redundancy-free spiking neural networks to rate networks

RING MODEL

For simplicity, in Fig. 1A, we simulate a ring model with spatially structured stochastic external input but without recurrent connections. For all $i = 1, \dots, N$,

$$\begin{aligned} \tau \frac{d}{dt} x_i(t) &= -x_i(t) + I_i^{\text{ext}}(t), \\ I_i^{\text{ext}}(t) &= \cos \left(2\pi \left(\frac{i}{N} + \Theta(t) \right) \right) \end{aligned}$$

with

$$\frac{d}{dt} \Theta(t) = \tilde{\sigma} \eta(t),$$

where $\eta(t)$ is a Gaussian white noise and $\tilde{\sigma} = 10^{-3}$.

FROM LOW-RANK SNNS TO NEURAL FIELD EQUATIONS

For any number of neurons N and any number of patterns p , let ξ be a random $N \times p$ -matrix with *i.i.d.*, zero-mean, unit-variance, normally distributed entries $\{\xi_{i\mu}\}_{i,\mu}$. We choose a connectivity matrix given by

$$J_{ij} := \frac{1}{cN} \sum_{\mu=1}^p \xi_{i\mu} (\phi(\xi_{j\mu}) - a) \quad \text{for all } i \neq j,$$

and $J_{ii} := 0$ for all i . As in the main text, $a := \int_{-\infty}^{\infty} \mathcal{D}z \phi(z)$ and $c := \int_{-\infty}^{\infty} \mathcal{D}z (\phi(z) - a)^2$, where $\mathcal{D}z$ is the standard Gaussian measure $\mathcal{D}z = dz$. This type of connectivity matrices was introduced by Brunel and Pereira [S1] in the context of Hopfield networks.

When the number of patterns p is kept constant as the number of neurons N tends to infinity, we say that the connectivity matrix $\mathbf{J} = \{J_{ij}\}_{\substack{1 \leq i \leq N \\ 1 \leq j \leq N}}$ is low-rank since it has finite rank p as $N \rightarrow \infty$. Although large, random, low-rank networks of neurons are not usually presented as spatially structured networks [S3, S4], they do have an implicit spatial structure. By identifying this spatial structure, we can derive exact neural field equations describing the dynamics of large networks, as we show here for the connectivity matrix \mathbf{J} .

For simplicity, let us first consider an SNN of N neurons without external input. The N neurons are assigned to N points in \mathbb{R}^p corresponding to the rows of ξ , i.e., neuron i is assigned to the point $\xi_i = (\xi_{i1}, \dots, \xi_{ip})$. Writing $u(t, \xi_i) = h_i(t)$ for all $i = 1, \dots, N$, we can interpret $u(t, \xi_i)$ as being the potential of a neuron at location $\xi_i \in \mathbb{R}^p$ at time t . Without loss of generality, let us consider the dynamics of neuron $i = 1$, which can be rewritten

$$\begin{aligned} \tau \frac{d}{dt} u(t, \xi_1) &= -u(t, \xi_1) + \underbrace{\sum_{j=2}^N \frac{1}{cN} \sum_{\mu=1}^p \xi_{1\mu} (\phi(\xi_{j\mu}) - a) s_j(t)}_{=J_{1j}}, \\ &= -u(t, \xi_1) + \frac{1}{c} \sum_{\mu=1}^p \xi_{1\mu} \frac{1}{N} \sum_{j=2}^N (\phi(\xi_{j\mu}) - a) s_j(t), \end{aligned}$$

where $s_j(t)$ has instantaneous firing rate $u(t, \xi_j)$. By spatial averaging [S5, S6], we have

$$\begin{aligned}
\lim_{N \rightarrow \infty} \frac{1}{N} \sum_{j=2}^N (\phi(\xi_{j\mu}) - a) s_j(t) &= \lim_{N \rightarrow \infty} \frac{1}{N} \sum_{j=2}^N (\phi(\xi_{j\mu}) - a) \phi(u(t, \xi_j)) \\
&= \int_{\mathbb{R}^d} \underbrace{\lim_{N \rightarrow \infty} \frac{1}{N} \sum_{j=2}^N \delta_{\xi_j}(d\mathbf{z})}_{=\mathcal{D}\mathbf{z}} (\phi(z_\mu) - a) \phi(u(t, \mathbf{z})) \\
&= \int_{\mathbb{R}^d} \mathcal{D}\mathbf{z} (\phi(z_\mu) - a) \phi(u(t, \mathbf{z})), \tag{S1}
\end{aligned}$$

where $\mathcal{D}\mathbf{z}$ denotes the p -dimensional standard Gaussian measure

$$\mathcal{D}\mathbf{z} = dz_1 \dots dz_p \frac{1}{(2\pi)^{p/2}} e^{-\|\mathbf{z}\|_2^2}.$$

Intuitively, the equalities (S1) simply reflect the fact that as $N \rightarrow \infty$, the empirical measure $\frac{1}{N} \sum_{i=1}^N \delta_{\xi_i}$ on \mathbb{R}^p , which summarizes the locations $\xi_1, \xi_2, \dots, \xi_N$ of neurons in \mathbb{R}^p , converges to the standard Gaussian measure $\mathcal{D}\mathbf{z}$ on \mathbb{R}^p (since the p -dimensional random vectors $\xi_1, \xi_2, \dots, \xi_N$ are *i.i.d.* with distribution $\mathcal{D}\mathbf{z}$), turning the summation over neurons into an integration over a Gaussian measure. Then, since the spatial distribution of neurons in \mathbb{R}^p converges to a continuous Gaussian distribution as $N \rightarrow \infty$, we get that the continuous field $u(t, \mathbf{y})$, with $\mathbf{y} \in \mathbb{R}^p$, solves the integro-differential equation

$$\tau \frac{\partial}{\partial t} u(t, \mathbf{y}) = -u(t, \mathbf{y}) + \frac{1}{c} \sum_{\mu=1}^p y_\mu \int_{\mathbb{R}^p} \mathcal{D}\mathbf{z} (\phi(z_\mu) - a) \phi(u(t, \mathbf{z})), \quad \forall \mathbf{y} \in \mathbb{R}^p.$$

Defining the connectivity kernel $w : \mathbb{R}^p \rightarrow \mathbb{R}^p$

$$w(\mathbf{y}, \mathbf{z}) := \frac{1}{c} \sum_{\mu=1}^p y_\mu (\phi(z_\mu) - a), \tag{S2}$$

we get a neural field equation [S2]:

$$\tau \frac{\partial}{\partial t} u(t, \mathbf{y}) = -u(t, \mathbf{y}) + \int_{\mathbb{R}^p} \mathcal{D}\mathbf{z} w(\mathbf{y}, \mathbf{z}) \phi(u(t, \mathbf{z})), \quad \forall \mathbf{y} \in \mathbb{R}^p. \tag{S3}$$

While the arguments presented here are informal, the neural field equation is the exact mean-field limit of the low-rank SNN: using the embedding of the low-rank SNN in \mathbb{R}^p , the convergence of the SNN to the neural field equation (S3) is guaranteed by rigorous results for spatially structured SNNs [S7].

Of course, by the same arguments, the corresponding low-rank RNN also converges to the neural field equation (S3).

In the case where half of the neurons receive an external input, as defined in the main text, we can also describe the population dynamics with neural field equations. Following the same steps as above, we get that for all neuron i receiving external input, $\lim_{N \rightarrow \infty} h_i^{\text{in}}(t) = \lim_{N \rightarrow \infty} x_i^{\text{in}}(t) = u^{\text{in}}(t, \xi_i)$, and for all neuron i' receiving no external input but only recurrent input, $\lim_{N \rightarrow \infty} h_{i'}^{\text{rec}}(t) = \lim_{N \rightarrow \infty} x_{i'}^{\text{rec}}(t) = u^{\text{rec}}(t, \xi_{i'})$, where the fields u^{in} and u^{rec} are the solutions to the system

$$\begin{aligned}
\tau \frac{\partial}{\partial t} u^{\text{in}}(t, \mathbf{y}) &= -u^{\text{in}}(t, \mathbf{y}) + \frac{1}{2} \int_{\mathbb{R}^p} \mathcal{D}\mathbf{z} w(\mathbf{y}, \mathbf{z}) \phi(u^{\text{in}}(t, \mathbf{z})) \\
&\quad + \frac{1}{2} \int_{\mathbb{R}^p} \mathcal{D}\mathbf{z} w(\mathbf{y}, \mathbf{z}) \phi(u^{\text{rec}}(t, \mathbf{z})) + \frac{\sigma}{\sqrt{p}} \sum_{\mu=1}^p y_\mu \eta_\mu(t), \quad \forall \mathbf{y} \in \mathbb{R}^p, \\
\tau \frac{\partial}{\partial t} u^{\text{rec}}(t, \mathbf{y}) &= -u^{\text{in}}(t, \mathbf{y}) + \frac{1}{2} \int_{\mathbb{R}^p} \mathcal{D}\mathbf{z} w(\mathbf{y}, \mathbf{z}) \phi(u^{\text{in}}(t, \mathbf{z})) \\
&\quad + \frac{1}{2} \int_{\mathbb{R}^p} \mathcal{D}\mathbf{z} w(\mathbf{y}, \mathbf{z}) \phi(u^{\text{rec}}(t, \mathbf{z})), \quad \forall \mathbf{y} \in \mathbb{R}^p,
\end{aligned}$$

CONCENTRATION OF THE ℓ^2 NORMS OF THE INCOMING WEIGHTS

To show that when the number of patterns p grows linearly with N , i.e., $p = \alpha N$ for some fixed $\alpha > 0$, the ℓ^2 norm of the incoming synaptic weights of any neuron i ,

$$\|\mathbf{J}_i\|_2 = \sqrt{\sum_{j=1}^N J_{ij}^2},$$

converges to $\sqrt{\alpha/c}$ as $N \rightarrow \infty$, we will show that, for any i ,

$$\lim_{N \rightarrow \infty} \mathbb{E}_{\xi} \left[\|\mathbf{J}_i\|_2^2 \right] = \frac{\alpha}{c} \quad (\text{S4})$$

and

$$\text{Var}_{\xi} \left(\|\mathbf{J}_i\|_2^2 \right) = \frac{2\alpha(1+\alpha)}{c^2 N} + \mathcal{O} \left(\frac{1}{N^2} \right), \quad (\text{S5})$$

where \mathbb{E}_{ξ} and Var_{ξ} denote, respectively, the expectation and the variance over the quenched disorder ξ . The fact that the variance scale as $\mathcal{O}(1/N)$ as $N \rightarrow \infty$ indicates that the random variable $\|\mathbf{J}_i\|_2^2$ indeed concentrates around α/c as $N \rightarrow \infty$. Without loss of generality, we can compute the expectation and the variance of $\|\mathbf{J}_1\|_2^2$. For any N ,

$$\begin{aligned} \mathbb{E}_{\xi} \left[\|\mathbf{J}_1\|_2^2 \right] &= \mathbb{E}_{\xi} \left[\sum_{j=1}^N J_{1j}^2 \right] = \sum_{j=1}^N \mathbb{E}_{\xi} \left[J_{1j}^2 \right] = \frac{1}{c^2 N^2} \sum_{j=2}^N \mathbb{E}_{\xi} \left[\left(\sum_{\mu=1}^p \xi_{1\mu} (\phi(\xi_{j\mu}) - a) \right)^2 \right] \\ &\stackrel{(*)}{=} \frac{1}{c^2 N^2} \sum_{j=2}^N \mathbb{E}_{\xi} \left[\sum_{\mu=1}^p \xi_{1\mu}^2 (\phi(\xi_{j\mu}) - a)^2 \right] = \frac{1}{c^2 N^2} \sum_{j=2}^N \sum_{\mu=1}^p \mathbb{E}_{\xi} \left[\xi_{1\mu}^2 (\phi(\xi_{j\mu}) - a)^2 \right] \\ &= \frac{1}{c^2 N^2} (N-1)\alpha N c \xrightarrow[N \rightarrow \infty]{} \frac{\alpha}{c} \end{aligned}$$

For the equality $(*)$, we used the fact that the cross terms are null since the columns of the random matrix ξ , i.e., the patterns, are independent and, when $\mu \neq \nu$,

$$\mathbb{E}_{\xi} \left[\xi_{1\mu} (\phi(\xi_{j\mu}) - a) \xi_{1\nu} (\phi(\xi_{j\nu}) - a) \right] = \mathbb{E}_{\xi} \left[\xi_{1\mu} (\phi(\xi_{j\mu}) - a) \right] \mathbb{E}_{\xi} \left[\xi_{1\nu} (\phi(\xi_{j\nu}) - a) \right] = 0.$$

For the variance, we have

$$\text{Var}_{\xi} \left(\|\mathbf{J}_1\|_2^2 \right) = \text{Var}_{\xi} \left(\sum_{j=1}^N J_{1j}^2 \right) = \mathbb{E}_{\xi} \left[\left(\sum_{j=1}^N J_{1j}^2 \right)^2 \right] - \mathbb{E}_{\xi} \left[\sum_{j=1}^N J_{1j}^2 \right]^2. \quad (\text{S6})$$

By the computation of the expectation above,

$$\mathbb{E}_{\xi} \left[\sum_{j=1}^N J_{1j}^2 \right]^2 = \frac{1}{c^2} \frac{(N-1)^2 p^2}{N^4}. \quad (\text{S7})$$

The second moment can be decomposed as

$$\begin{aligned} \mathbb{E}_{\xi} \left[\left(\sum_{j=1}^N J_{1j}^2 \right)^2 \right] &= \mathbb{E}_{\xi} \left[\sum_{j=1}^N J_{1j}^4 + \sum_{j=1}^N \sum_{k \neq j} J_{1j}^2 J_{1k}^2 \right] \\ &= (N-1) \mathbb{E}_{\xi} \left[J_{12}^4 \right] + (N-1)(N-2) \mathbb{E}_{\xi} \left[J_{12}^2 J_{13}^2 \right], \end{aligned} \quad (\text{S8})$$

and we compute the terms $\mathbb{E}_{\xi} [J_{12}^4]$ and $\mathbb{E}_{\xi} [J_{12}^2 J_{13}^2]$ separately.

$$\begin{aligned}
\mathbb{E}_{\xi} [J_{12}^4] &= \frac{1}{c^4 N^4} \mathbb{E}_{\xi} \left[\left(\sum_{\mu=1}^p \xi_{1\mu} (\phi(\xi_{2\mu}) - a) \right)^4 \right] \\
&\stackrel{(*)}{=} \frac{1}{c^4 N^4} \sum_{\mu=1}^p \mathbb{E}_{\xi} \left[\xi_{1\mu}^4 (\phi(\xi_{2\mu}) - a)^4 \right] \\
&\quad + \frac{1}{c^4 N^4} \sum_{1 \leq \mu < \nu \leq p} \binom{4}{2} \mathbb{E}_{\xi} \left[\xi_{1\mu}^2 (\phi(\xi_{2\mu}) - a)^2 \xi_{1\nu}^2 (\phi(\xi_{2\nu}) - a)^2 \right] \\
&= \mathcal{O} \left(\frac{1}{N^3} \right) + \frac{1}{c^4 N^4} \frac{p(p-1)}{2} 6c^2 \\
&= \frac{3}{c^2 N^4} p(p-1) + \mathcal{O} \left(\frac{1}{N^3} \right), \tag{S9}
\end{aligned}$$

where for equality (*), we used the fact that, in the multinomial expansion of

$$\mathbb{E}_{\xi} \left[\left(\sum_{\mu=1}^p \xi_{1\mu} (\phi(\xi_{2\mu}) - a) \right)^4 \right],$$

all terms with at least one odd power are null. Similarly,

$$\begin{aligned}
\mathbb{E}_{\xi} [J_{12}^2 J_{13}^2] &= \frac{1}{c^4 N^4} \mathbb{E}_{\xi} \left[\left(\sum_{\mu=1}^p \xi_{1\mu} (\phi(\xi_{2\mu}) - a) \right)^2 \left(\sum_{\mu=1}^p \xi_{1\mu} (\phi(\xi_{3\mu}) - a) \right)^2 \right] \\
&= \frac{1}{c^4 N^4} \sum_{\mu=1}^p \mathbb{E}_{\xi} \left[\xi_{1\mu}^4 (\phi(\xi_{2\mu}) - a)^2 (\phi(\xi_{3\mu}) - a)^2 \right] \\
&\quad + \frac{2}{c^4 N^4} \sum_{1 \leq \mu < \nu \leq p} \mathbb{E}_{\xi} \left[\xi_{1\mu}^2 (\phi(\xi_{2\mu}) - a)^2 \xi_{1\nu}^2 (\phi(\xi_{3\nu}) - a)^2 \right] \\
&= \frac{1}{c^4 N^4} p 3c^2 + \frac{2}{c^4 N^4} \frac{p(p-1)}{2} c^2 \\
&= \frac{3}{c^2 N^4} p + \frac{1}{c^2 N^4} p(p-1). \tag{S10}
\end{aligned}$$

From Eqs (S6), (S7), (S8), (S9) and (S10), we get

$$\begin{aligned}
\text{Var} (\|\mathbf{J}_1\|_2^2) &= \mathbb{E} \left[\left(\sum_{j=1}^N J_{ij}^2 \right)^2 \right] - \mathbb{E} \left[\sum_{j=1}^N J_{ij}^2 \right]^2 \\
&= (N-1) \mathbb{E} [J_{12}^4] + (N-1)(N-2) \mathbb{E} [J_{12}^2 J_{13}^2] - \frac{1}{c^2 N^4} (N-1)^2 p^2 \\
&= \frac{3}{c^2} \frac{(N-1)p(p-1)}{N^4} \\
&\quad + \frac{3}{c^2} \frac{(N-1)(N-2)p}{N^4} + \frac{1}{c^2} \frac{(N-1)(N-2)p(p-1)}{N^4} \\
&\quad - \frac{1}{c^2} \frac{(N-1)^2 p^2}{N^4} + \mathcal{O} \left(\frac{1}{N^2} \right).
\end{aligned}$$

Using the fact that

$$\begin{aligned}
(N-1)^2 p^2 &= (N-1)(N-2)p^2 + (N-1)p^2 \\
&= (N-1)(N-2)p(p-1) + (N-1)(N-2)p + (N-1)p(p-1) + (N-1)p,
\end{aligned}$$

and after some rearrangement of terms, we obtain

$$\text{Var} \left(\|\mathbf{J}_1\|_2^2 \right) = \frac{2\alpha(1+\alpha)}{c^2 N} + \mathcal{O} \left(\frac{1}{N^2} \right).$$

FEEDFORWARD NETWORK APPROXIMATION

To understand better the dynamics of the input-driven disordered network model, we approximate the recurrent SNN and the RNN by a feedforward SNN and a feedforward rate network, respectively. Before introducing the feedforward networks, let us first rewrite the dynamics of the SNN in a more mathematical form, which will help us to better disentangle the three independent sources of noise present in the model: the quenched disorder ξ , the input external noise $\{\eta_\mu\}_{\mu=1}^p$, and neuronal spike noise. Let $\{\pi_i\}_{i=1}^N$ be a collection of N independent Poisson random measures on $\mathbb{R}_+ \times \mathbb{R}_+$ with unit intensity. The dynamics of the SNN (Equation (1) in the main text) can be rewritten as a system of stochastic differential equations: for all $i = 1, \dots, N$,

$$\tau dh_i(t) = -h_i(t)dt + \sum_{j=1}^N J_{ij}dZ_j(t) + I_i^{\text{ext}}(t)dt, \quad (\text{S11a})$$

$$Z_i(t) = \int_{[0,t] \times \mathbb{R}_+} \mathbb{1}_{z \leq \phi(h_i(s-))} \pi_i(ds, dz). \quad (\text{S11b})$$

Formally, the spike train of neuron i , $S_i(t) = \sum_k \delta(t - t_i^k)$ (where the $\{t_i^k\}_k$ are the spike times of neuron i), is simply $S_i(t) = dZ_i(t)/dt$. The mathematical notation (S11a), while less common in the theoretical neuroscience literature than Equation (1) in the main text, has the important advantage of clearly separating intrinsic neuronal noise, which stems from the biophysics of single neurons and which is independent from one neuron to another, from other sources of noise. Here, intrinsic neuronal spike noise is modeled by the independent Poisson random measures π_i . As stated in the main text, conditioned on the potentials $\{h_i(t)\}_{i=1}^N$, the processes $\{S_i(t) = dZ_i(t)/dt\}_{i=1}^N$ are independent inhomogeneous Poisson processes with instantaneous firing rates $\{\phi(h_i(t))\}_{i=1}^N$. The notation $h_i(s-)$ in Eq. (S11b) represents the left limit $\lim_{u \uparrow s} h_i(u)$ and indicates that the dynamics are defined in terms of Itô calculus. Consistently, in the input-driven model (with external input defined by Equation (6) in the main text), we replace the p independent Gaussian white noises $\{\eta_\mu(t)\}_{\mu=1}^p$ of the external inputs by p independent standard Brownian motions $\{B_\mu(t)\}_{\mu=1}^p$: for all $i \leq N/2$ (neurons receiving external input),

$$I_i^{\text{ext}}(t)dt = \frac{\sigma}{\sqrt{p}} \sum_{\mu=1}^p \xi_{i\mu} \eta_\mu(t)dt = \frac{\sigma}{\sqrt{p}} \sum_{\mu=1}^p \xi_{i\mu} dB_\mu(t).$$

For indexing convenience, let us write $\{h_i^{\text{in}}(t) := h_i(t)\}_{i=1}^{N/2}$ the potentials of the $N/2$ neurons receiving external input and $\{h_i^{\text{rec}}(t) := h_{N/2+i}(t)\}_{i=1}^{N/2}$ the potentials of the $N/2$ neurons receiving no external input but only recurrent input. By neglecting all the recurrent connections except for those from neurons receiving external input, $\{h_i^{\text{in}}(t)\}_{i=1}^{N/2}$, to neurons receiving no external input but only recurrent input, $\{h_i^{\text{rec}}(t)\}_{i=1}^{N/2}$, we get a feedforward SNN where the neurons of a first layer, $\{h_i^{(1)}(t) \approx h_i^{\text{in}}(t)\}_{i=1}^{N/2}$, receive external input and the neurons of a second layer, $\{h_i^{(2)}(t) \approx h_i^{\text{rec}}(t)\}_{i=1}^{N/2}$, receive inputs from the first; cf Fig. S1. For all neurons i in the first layer of the feedforward SNN, the stochastic spike activity is given

$$\tau dh_i^{(1)}(t) = -h_i^{(1)}(t)dt + \frac{\sigma}{\sqrt{p}} \sum_{\mu=1}^p \xi_{i\mu} dB_\mu(t), \quad (\text{S12a})$$

$$Z_i^{(1)}(t) = \int_{[0,t] \times \mathbb{R}_+} \mathbb{1}_{z \leq \phi(h_i^{(1)}(s-))} \pi_i(ds, dz), \quad (\text{S12b})$$

and for all neurons i in the second layer of the feedforward SNN, the potential dynamics follows

$$\tau dh_i^{(2)}(t) = -h_i^{(2)}(t)dt + \sum_{j=1}^{N/2} J_{ij} dZ_j^{(1)}(t). \quad (\text{S12c})$$

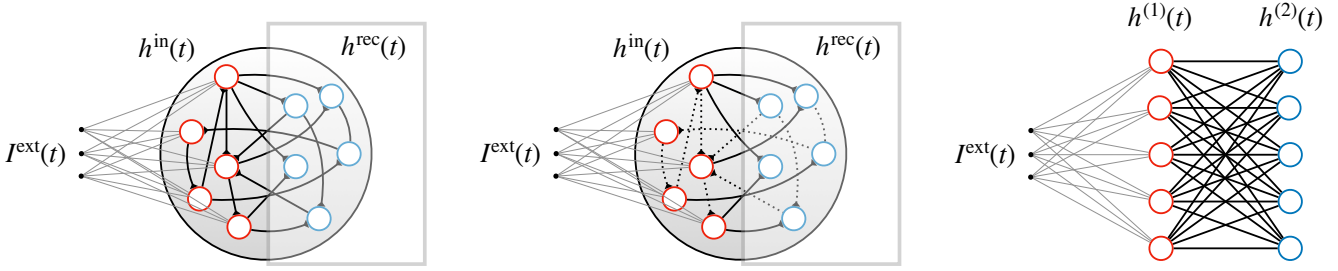


FIG. S1. Feedforward network approximation of the input-driven model.

In Eq. (S12) we see distinctly the three independent sources of noise: the quenched disorder ξ , the external input noise $\{B_\mu(t)\}_{\mu=1}^p$ (independent Brownian motions), and the neuronal spike noise $\{\pi_i\}_{i=1}^{N/2}$ (independent Poisson random measures).

Analogously, the feedforward rate network reads

$$\tau dx_i^{(1)}(t) = -x_i^{(1)}(t)dt + \frac{\sigma}{\sqrt{p}} \sum_{\mu=1}^p \xi_{i\mu} dB_\mu(t), \quad i = 1, \dots, N/2, \quad (\text{S13a})$$

$$\tau \frac{d}{dt} x_i^{(2)}(t) = -x_i^{(2)}(t) + \sum_{j=1}^{N/2} J_{ij} \phi(x_j^{(1)}(t)), \quad i = 1, \dots, N/2. \quad (\text{S13b})$$

Note in the feedforward network approximations Eq. (S12) and Eq. (S13), the potentials of the first layers $h_i^{(1)}(t)$ and $x_i^{(1)}(t)$ are equal since they integrate the same external input $\frac{\sigma}{\sqrt{p}} \sum_{\mu=1}^p \xi_{i\mu} dB_\mu(t)$.

The approximations $h_i^{(1)}(t) \approx h_i^{\text{in}}(t)$ and $h_i^{(2)}(t) \approx h_i^{\text{rec}}(t)$ (as well as the approximations $x_i^{(1)}(t) \approx x_i^{\text{in}}(t)$ and $x_i^{(2)}(t) \approx x_i^{\text{rec}}(t)$) are not exact, however, since the disordered networks are in an input-driven regime, the feedforward network approximation provides some intuition about two non-trivial numerical facts:

1. The correlation between neurons is given by the disorder ξ , i.e.,

$$\rho(h_i^{\text{rec}}, h_j^{\text{rec}}) \approx \frac{1}{p} \sum_{\mu=1}^p \xi_{i\mu} \xi_{j\mu}.$$

2. The distance between large SNNs and large RNNs, $\Delta^{\text{rec}}(\alpha)$, scale as $\mathcal{O}(\sqrt{\alpha})$ as $\alpha \rightarrow 0$.

We recall that the distance $\Delta^{\text{rec}}(\alpha)$ is defined as the average distance over time

$$\Delta^{\text{rec}}(\alpha) := \lim_{T \rightarrow \infty} \frac{1}{T} \int_0^T \left| \hat{h}_{i^*}^{\text{rec}}(t) - \hat{x}_{i^*}^{\text{rec}}(t) \right| dt,$$

where $\hat{h}_{i^*}^{\text{rec}}(t)$ is the potential of a typical neuron i^* in a large SNN and $\hat{x}_{i^*}^{\text{rec}}(t)$ the corresponding potential in the large RNN and that the heuristic argument presented in the main text (see Equation (9) in the main text) only deals with and infinitesimally short time interval. While proving 1. and 2. on the fully recurrent network is challenging, the feedforward network approximations, Eq. (S12) and Eq. (S13), are much more tractable. Therefore, instead of proving 1. and 2., we will only show, on the feedforward network approximations, that

$$1'. \rho(h_i^{(1)}(t), h_j^{(1)}(t)) \approx \frac{1}{p} \sum_{\mu=1}^p \xi_{i\mu} \xi_{j\mu}.$$

$$2'. \text{When } N \rightarrow \infty, \text{ for any } i, \lim_{T \rightarrow \infty} \frac{1}{T} \int_0^T |h_i^{(2)}(t) - x_i^{(2)}(t)| dt = \mathcal{O}(\sqrt{\alpha}), \text{ as } \alpha \rightarrow 0.$$

1. Correlation between neurons

Here, we show point 1'. In the following, we always assume that at time $t = 0$, all the potentials are zero, i.e.,

$$h_i^{(1)}(0) = x_i^{(1)}(0) = h_i^{(2)}(0) = x_i^{(2)}(0) = 0, \quad \forall i.$$

This choice of initial condition has no consequence, except that it simplifies calculations, since the effect of the initial condition vanishes as $t \rightarrow +\infty$ (potentials are leaky integrators and the networks have a feedforward architecture).

Integrating Eq. (S12a), we get

$$\begin{aligned} h_i^{(1)}(t) &= \int_0^t \frac{1}{\tau} e^{-(t-s)/\tau} I_i^{\text{ext}}(s) ds = \int_0^t \frac{1}{\tau} e^{-(t-s)/\tau} \frac{\sigma}{\sqrt{p}} \sum_{\mu=1}^p \xi_{i\mu} dB_{\mu}(s) \\ &= \frac{\sigma}{\sqrt{p}} \sum_{\mu=1}^p \xi_{i\mu} \underbrace{\int_0^t \frac{1}{\tau} e^{-(t-s)/\tau} dB_{\mu}(s)}_{\sim \mathcal{N}\left(0, \frac{1}{2\tau}(1-e^{-2t/\tau})\right)} \end{aligned}$$

Where $\mathcal{N}\left(0, \frac{1}{2\tau}(1-e^{-2t/\tau})\right)$ denotes the law of a zero-mean normal variable with variance $\frac{1}{2\tau}(1-e^{-2t/\tau})$.

By ergodicity (the average over time of a realization of the process is equal to the average over the stationary distribution of the process),

$$\begin{aligned} \overline{h_i^{(1)}} &:= \lim_{T \rightarrow \infty} \frac{1}{T} \int_0^T h_i(t) dt = \lim_{T \rightarrow \infty} \mathbb{E}_{\{B_{\mu}\}_{\mu=1}^p} \left[h_i^{(1)}(T) \right] \\ &= \lim_{T \rightarrow \infty} \frac{\sigma}{\sqrt{p}} \sum_{\mu=1}^p \xi_{i\mu} \underbrace{\mathbb{E}_{B_{\mu}} \left[\int_0^T \frac{1}{\tau} e^{-(T-t)/\tau} dB_{\mu}(t) \right]}_{=0} = 0, \end{aligned}$$

and

$$\begin{aligned} \sigma_{h_i^{(1)}}^2 &:= \lim_{T \rightarrow \infty} \frac{1}{T} \int_0^T (h_i^{(1)}(t) - \overline{h_i^{(1)}})^2 dt \\ &= \lim_{T \rightarrow \infty} \mathbb{E}_{\{B_{\mu}\}_{\mu=1}^p} \left[\left(\frac{\sigma}{\sqrt{p}} \sum_{\mu=1}^p \xi_{i\mu} \int_0^T \frac{1}{\tau} e^{-(T-t)/\tau} dB_{\mu}(t) \right)^2 \right] \\ &\stackrel{(*)}{=} \frac{\sigma^2}{p} \sum_{\mu=1}^p \xi_{i\mu}^2 \underbrace{\lim_{T \rightarrow \infty} \mathbb{E}_{B_{\mu}} \left[\left(\int_0^T \frac{1}{\tau} e^{-(T-t)/\tau} dB_{\mu}(t) \right)^2 \right]}_{= \frac{1}{2\tau}(1-e^{-2t^T/\tau})} = \frac{\sigma^2}{2\tau p} \sum_{\mu=1}^p \xi_{i\mu}^2, \end{aligned}$$

where for the equality (*), we use the fact that the cross terms are null because the Brownian motions $\{B_{\mu}\}_{\mu=1}^p$ are independent and, when $\mu \neq \nu$,

$$\begin{aligned} \mathbb{E}_{\{B_{\mu}, B_{\nu}\}} \left[\left(\int_0^T \frac{1}{\tau} e^{-(T-t)/\tau} dB_{\mu}(t) \right) \left(\int_0^T \frac{1}{\tau} e^{-(T-t)/\tau} dB_{\nu}(t) \right) \right] \\ = \mathbb{E}_{B_{\mu}} \left[\left(\int_0^T \frac{1}{\tau} e^{-(T-t)/\tau} dB_{\mu}(t) \right) \right] \mathbb{E}_{B_{\nu}} \left[\left(\int_0^T \frac{1}{\tau} e^{-(T-t)/\tau} dB_{\nu}(t) \right) \right] = 0. \end{aligned}$$

For any pair $i \neq j$,

$$\begin{aligned}
\rho(h_i^{(1)}, h_j^{(1)}) &:= \lim_{T \rightarrow \infty} \int_0^T \frac{(h_i^{(1)}(t) - \overline{h_i^{(1)}})(h_j^{(1)}(t) - \overline{h_j^{(1)}})}{\sigma_{h_i^{(1)}} \sigma_{h_j^{(1)}}} dt \\
&\stackrel{(*)}{=} \frac{1}{\sigma_{h_i^{(1)}} \sigma_{h_j^{(1)}}} \frac{\sigma^2}{p} \sum_{\mu=1}^p \xi_{i\mu} \xi_{j\mu} \lim_{T \rightarrow \infty} \mathbb{E}_{B_\mu} \left[\left(\int_0^T \frac{1}{\tau} e^{-(T-t)/\tau} dB_\mu(t) \right)^2 \right] \\
&= \frac{\frac{1}{p} \sum_{\mu=1}^p \xi_{i\mu} \xi_{j\mu}}{\sqrt{\frac{1}{p} \sum_{\mu=1}^p \xi_{i\mu}^2} \sqrt{\frac{1}{p} \sum_{\mu=1}^p \xi_{j\mu}^2}},
\end{aligned}$$

where for the equality $(*)$, we use again the fact the cross terms are null. When N is large, $\frac{1}{p} \sum_{\mu=1}^p \xi_{i\mu}^2 \approx 1$, whence the approximation

$$\rho(h_i^{(1)}, h_j^{(1)}) \approx \frac{1}{p} \sum_{\mu=1}^p \xi_{i\mu} \xi_{j\mu}.$$

2. Distance between large SNNs and large rate networks

Here, we show point 2'. For any i ,

$$\begin{aligned}
&\mathbb{E}_{\{\pi_j\}_{i=j}^{N/2}} \left[(h_i^{(2)}(t) - x_i^{(2)}(t))^2 \right] \\
&= \mathbb{E}_{\{\pi_j\}_{i=j}^{N/2}} \left[\left(\sum_{j=1}^{N/2} J_{ij} \int_0^t \frac{1}{\tau} e^{-(t-s)/\tau} dZ_j^{(1)}(s) - \sum_{j=1}^{N/2} J_{ij} \int_0^t \frac{1}{\tau} e^{-(t-s)/\tau} \phi(x_j^{(1)}(s)) ds \right)^2 \right] \\
&\stackrel{(*)}{=} \sum_{j=1}^{N/2} J_{ij}^2 \mathbb{E}_{\pi_j} \left[\left(\int_0^t \frac{1}{\tau} e^{-(t-s)/\tau} dZ_j^{(1)}(s) - \int_0^t \frac{1}{\tau} e^{-(t-s)/\tau} \phi(x_j^{(1)}(s)) ds \right)^2 \right] \\
&= \sum_{j=1}^{N/2} J_{ij}^2 \int_0^t \left(\frac{1}{\tau} e^{-(t-s)/\tau} \right)^2 \underbrace{\phi(x_j^{(1)}(s)) ds}_{\leq \|\phi\|_\infty} \leq \sum_{j=1}^{N/2} J_{ij}^2 \frac{1}{2\tau} (1 - e^{-t/\tau}) \|\phi\|_\infty,
\end{aligned}$$

where for the equality $(*)$, we use the fact that the cross terms are null because the Poisson random measures $\{\pi_j^{(1)}\}_{j=1}^{N/2}$ are independent and, for all $j = 1, \dots, N/2$,

$$\mathbb{E}_{\pi_j} \left[\int_0^t \frac{1}{\tau} e^{-(t-s)/\tau} dZ_j^{(1)}(s) - \int_0^t \frac{1}{\tau} e^{-(t-s)/\tau} \phi(x_j^{(1)}(s)) ds \right] = 0.$$

Just as an aside, in the main text, we have always assumed that the bound $\|\phi\|_\infty = \max_x |\phi(x)|$ was smaller or equal to $1/\tau$.

By ergodicity,

$$\begin{aligned}
&\lim_{T \rightarrow \infty} \frac{1}{T} \int_0^T |h_i^{(2)}(t) - x_i^{(2)}(t)| dt \\
&= \lim_{T \rightarrow \infty} \mathbb{E}_{\{\pi_j\}_{j=1}^{N/2}, \{B_\mu\}_{\mu=1}^p} \left[|h_i^{(2)}(T) - x_i^{(2)}(T)| \right] \\
&\leq \lim_{T \rightarrow \infty} \mathbb{E}_{\{\pi_j\}_{j=1}^{N/2}, \{B_\mu\}_{\mu=1}^p} \left[(h_i^{(2)}(T) - x_i^{(2)}(T))^2 \right]^{1/2} \\
&= \lim_{T \rightarrow \infty} \mathbb{E}_{\{\pi_j\}_{j=1}^{N/2}, \{B_\mu\}_{\mu=1}^p} \left[\mathbb{E}_{\{\pi_j\}_{j=1}^{N/2}} \left[(h_i^{(2)}(T) - x_i^{(2)}(T))^2 | \{B_\mu\}_{\mu=1}^p \right] \right]^{1/2}
\end{aligned}$$

But as noticed above,

$$\mathbb{E}_{\{\pi_j\}_{j=1}^{N/2}} \left[\left(h_i^{(2)}(T) - x_i^{(2)}(T) \right)^2 | \{B_\mu\}_{\mu=1}^p \right] \leq \frac{\|\phi\|_\infty}{2\tau} \sum_{j=1}^{N/2} J_{ij}^2.$$

Furthermore, by Eqs. (S4) and (S5),

$$\sum_{j=1}^{N/2} J_{ij}^2 \xrightarrow{N \rightarrow \infty} \frac{1}{2} \frac{\alpha}{c}$$

Hence, as $N \rightarrow \infty$, for any i ,

$$\lim_{T \rightarrow \infty} \frac{1}{T} \int_0^T \left| h_i^{(2)}(t) - x_i^{(2)}(t) \right| dt \leq \frac{1}{2} \sqrt{\frac{\|\phi\|_\infty}{\tau c}} \sqrt{\alpha},$$

which shows that the distance between large SNNs and large rate networks indeed scale as $\mathcal{O}(\sqrt{\alpha})$, as $\alpha \rightarrow 0$.

-
- [S1] Pereira, U. & Brunel, N. Attractor dynamics in networks with learning rules inferred from in vivo data. *Neuron*. (2018)
- [S2] Bressloff, P. Spatiotemporal dynamics of continuum neural fields. *Journal Of Physics A: Mathematical And Theoretical*. **45**, 033001 (2011)
- [S3] Schuessler, F., Dubreuil, A., Mastrogiovanni, F., Ostojic, S. & Barak, O. Dynamics of random recurrent networks with correlated low-rank structure. *Physical Review Research*. **2**, 013111 (2020)
- [S4] Mastrogiovanni, F. & Ostojic, S. Linking connectivity, dynamics, and computations in low-rank recurrent neural networks. *Neuron*. **99**, 609-623 (2018)
- [S5] Gerstner, W. Time structure of the activity in neural network models. *Phys. Rev. E*. **51**, 738 (1995)
- [S6] Gerstner, W., Kistler, W., Naud, R. & Paninski, L. *Neuronal dynamics: From single neurons to networks and models of cognition*. (Cambridge University Press, 2014)
- [S7] Chevallier, J., Duarte, A., Löcherbach, E. & Ost, G. Mean field limits for nonlinear spatially extended Hawkes processes with exponential memory kernels. *Stochastic Processes And Their Applications*. **129**, 1-27 (2019)